Analysis of photoluminescence from solubilized single-walled carbon nanotubes

Marcus Jones, Chaiwat Engtrakul, Wyatt K. Metzger, Randy J. Ellingson, Arthur J. Nozik, Michael J. Heben, and Garry Rumbles

Center for Basic Sciences, National Renewable Energy Laboratory, 1617 Cole Boulevard, Golden, Colorado, 80401-3393, USA

(Received 5 June 2004; revised manuscript received 27 October 2004; published 25 March 2005)

The functional form of the photoluminescence (PL) line shape from individual single-walled carbon nanotube (SWNT) species is found to contain a significant Lorentzian component and the Stokes shift is observed to be very small (<8 meV), which suggests an excitonic dephasing mechanism that is largely decoupled from surrounding solvent and surfactant molecules. The PL quantum yield (PLQY) of two SWNT species is determined to be $\sim 5\times 10^{-4}$, and it is suggested that this is lower than the "true" value due to quenching of the PL in bundles by metallic tubes. Time-resolved PL measurements reveal a dominant, luminescence lifetime component of 130 ps that, when combined with a predicted natural radiative lifetime of ~ 20 ns, suggests that the true PLQY is $\sim 6.5\times 10^{-3}$. Finally, deconvoluted PL excitation spectra are produced for eight SWNT species, and the appearance of a higher-energy excitonic subband is discussed.

DOI: 10.1103/PhysRevB.71.115426 PACS number(s): 73.61.Wp, 71.35.−y, 71.20.Tx

I. INTRODUCTION

Carbon nanotubes were discovered in 1991[1] and have been found to possess a wide variety of remarkable mechanical,[2] thermal,[3] and electrical[4–6] properties and have many potential practical applications. Recently, however, the discovery, by O'Connell *et al.*,[7] of structured near-infrared photoluminescence from suitably isolated semiconducting single-walled carbon nanotubes (SWNTs) has generated substantial interest in their optical properties. Since that report, steady-state photoluminescence spectra have been measured on aqueous suspensions of both HiPco SWNTs,[7–9] produced by gas-phase chemical vapor deposition in high pressure carbon monoxide[10] and SWNTs produced by pulsed laser vaporization of Ni/Co/carbon targets.[11,12] Photoluminescence efficiencies of HiPco tubes are found to reversibly decrease as pH is lowered[9] and fluorescence energies are changed [within a ~ 25 meV range for (8,3) tubes] when different surfactants are used to stabilize the SWNTs in solution.[13] In addition, SWNTs suspended in air between silicon pillars were found to exhibit room temperature PL[14,15] that was broadly similar to the PL from micellar suspensions. When individual nanotubes were probed, at 4 K[16] and 300 K,[17] a distribution of PL energies was found for tubes with common chiral symmetry and diameter, which likely arose from tube defects or variations in the local environment. Cryogenic studies have also shown the emergence of new PL peaks in the ensemble spectrum at low temperatures.[18]

Time-resolved measurements[19–26] have also been employed in an attempt to elucidate the carrier dynamics in photoexcited single-walled carbon nanotubes. Wavelength-dependent pump-probe spectroscopy has revealed a subpicosecond intraband relaxation and a longer[25] (5-20 ps) component that is attributed to interband carrier recombination. Measurements of SWNT fluorescence decay[22,24,26] have, until now, resulted in PL lifetime estimates of $\sim 10-15$ ps; however, in this paper we report lifetime values for three different tube species that are approximately 1 order of magnitude larger.

One electron band theory was initially used to explain SWNT spectra, but significant deviations were found between theory and experiment. For example, the ratio of the energy of the *second* peak in the excitation spectrum to the fluorescence energy was predicted to asymptotically approach 2 in the limit of the large tube radius; experimentally, it instead approaches an asymptotic value nearer to 1.75. The effects of electron-hole interactions in SWNTs, identified by Ando,[27] have recently been found to resolve the "ratio problem"[28] and the consideration of excitonic states in SWNTs has resulted in a more accurate description of SWNT electronic structure.[29,30]

This paper describes the results of a detailed analysis of the steady-state and time-resolved PL of aqueous suspensions of SWNTs. We illustrate the extraction of spectral information pertaining to a single-tube species within a highly polydisperse SWNT sample by examination of the two-dimensional (2D) PL landscape, whose boundaries are defined by excitation and emission wavelength vectors (λ_{ex} and λ_{em}). Absorption data are also presented, and accurate measurements of the Stoke's shift are reported for four-tube species. An estimate of the PL quantum yield (PLQY) is made for two individual SWNT species and this is found to be broadly in agreement with previous values for the ensemble PL. In addition, time-resolved fluorescence decays have been measured and analyzed, enabling an estimate of the natural fluorescence lifetime in SWNTs. Single species SWNT excitation spectra are generated from the results of the PL analysis and the observation of a high-energy excitonic subband is discussed.

II. EXPERIMENTAL SECTION

Using a method similar to one previously reported,[7] 12 mg of as-produced HiPco[10] SWNTs (Carbon Nanotechnologies) were suspended in 15 ml of aqueous sodium dodecyl sulfate (SDS) surfactant (1 wt %) using a cup-horn sonicator connected to an ultrasonic processor (Cole-Palmer, 750 W). The mixture was kept in a water bath cooled to

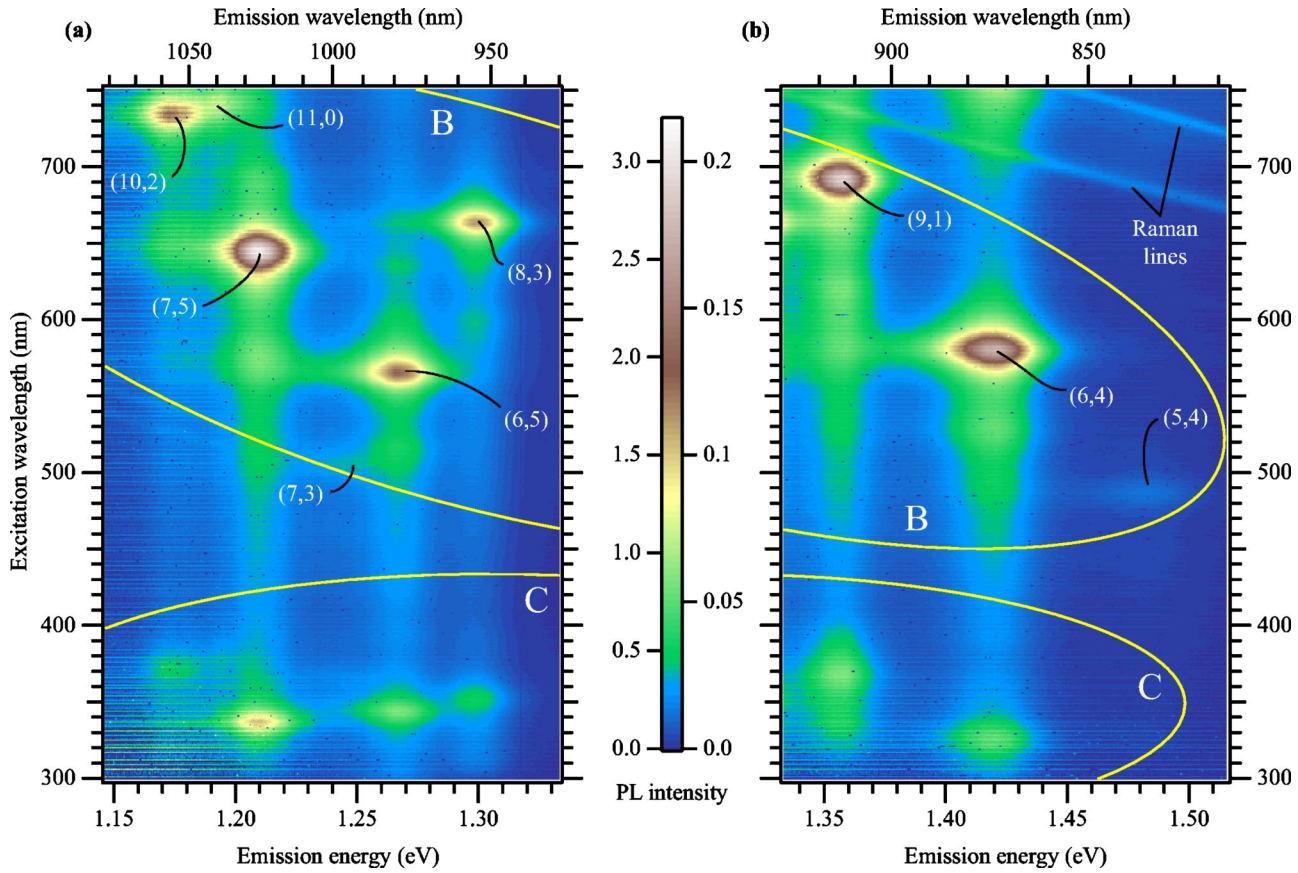

FIG. 1. (Color online) 2D PL spectrum of aqueous SWNTs. Images (a) and (b) are contiguous, but the intensity scale on image (b) is enhanced by a factor of 15 compared to that of image (a). The encircled areas, marked B and C, contain resonant PL peaks from SWNTs that have been excited to the B_0 and C_0 excitons, respectively.

15 °C during the sonication period (12 min). The resulting suspension was centrifuged (Beckman Coulter, Optima XL-100 K) at 104 000 g for 4 h using a swing bucket rotor (SW-28). A stable suspension of SWNTs was isolated by decanting the upper 75% of the supernatant and used for subsequent experiments.

Photoluminescence (PL) spectra were recorded using a Fluorolog-3 (JYHoriba) spectrometer that utilized a liquid-N_2-cooled charge-coupled-device (CCD) detector. Monochromatic excitation light was generated by a xenon arc lamp dispersed through a double monochromator. Fluorescence was collected perpendicular to the excitation beam, passed through a single monochromator containing a 300 line/mm grating and imaged on a cooled (80 K) CCD array. All PL spectra were corrected for the spectral output intensity of the excitation source and for the spectral response of the detection system. Linear absorption spectra were recorded on a Cary 500 double beam spectrophotometer at 1 nm spectral resolution.

Room-temperature PL decay curves were measured by time-correlated single-photon counting (TCSPC).[31] Photoexcitation at the desired wavelength was provided by an optical parametric amplifier pumped by the output of a titanium:sapphire laser system with a regenerative amplifier. The final laser output consisted of a 250 kHz pulse train with an average power of 5 mW, a spot size of about 2 mm, and a pulse width of several hundred femtoseconds. The SWNT PL, detected perpendicular to the excitation beam, was passed through long pass filters and a spectrometer (Spex 320M) and detected by a cooled (80 K), red-sensitive photomultiplier tube (Hamamatsu R5509). Instrument response functions (IRFs), with a width of ~200 ps, were measured using scattered light from the same samples as those from which fluorescence was viewed. Analysis of the PL decays was achieved by nonlinear least squares[32] iterative reconvolution of a model exponential decay function with the IRFs. This technique effectively removed the contribution of the IRF to the PL decay and resulted in a temporal response of ~20 ps, i.e., 10% of the instrument response function width.[31]

III. RESULTS AND DISCUSSION

Excitation of an SDS-water solution of SWNTs with λ_{ex} varied from 300 to 750 nm produced PL spectra that are presented in Fig. 1. Limitations of the sensitivity of the CCD detector in the near-infrared (near-IR) enabled only a subset of the total SWNT fluorescence to be recorded. The PL is associated with emission from the lowest SWNT electronic excited state and each peak is assigned an (n,m) symmetry label by referring to the empirical Kataura plot published by Weisman and Bachilo.[33] The two encircled areas, labeled B and C, contain PL peaks that occur after optically allowed

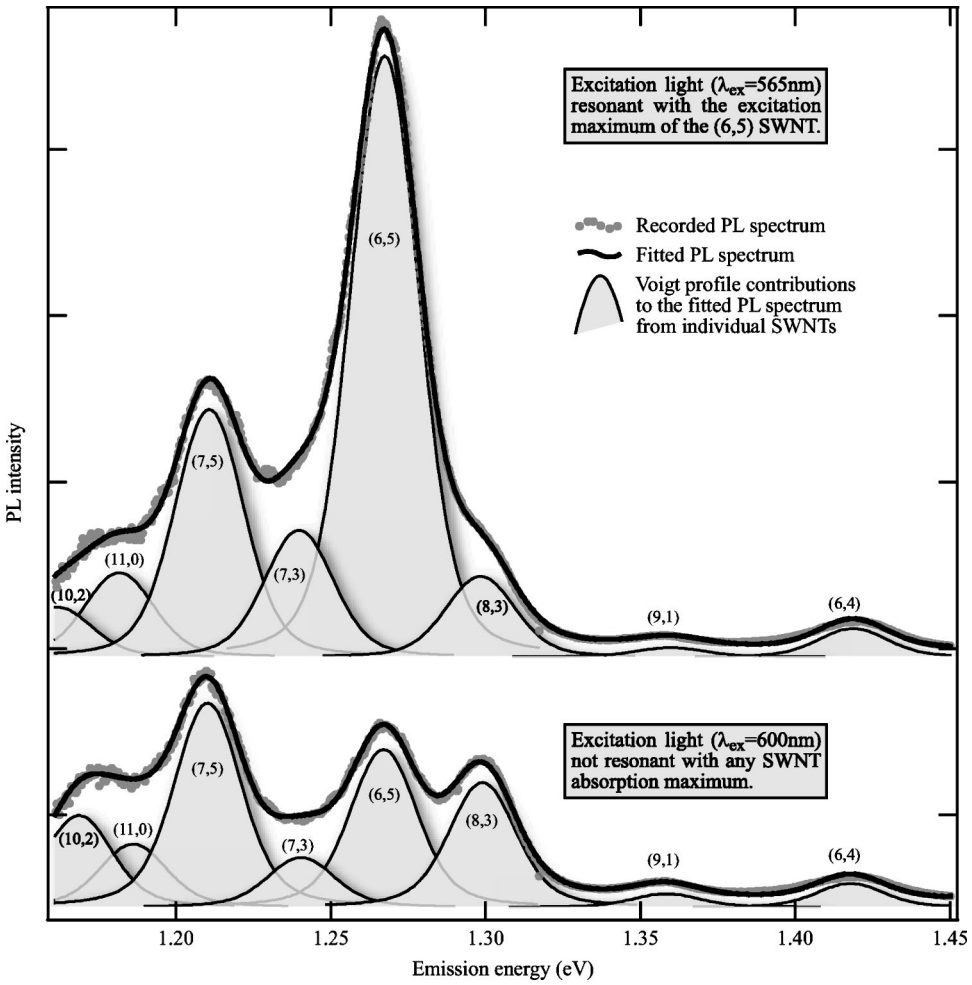

FIG. 2. Resonant (upper) and nonresonant (lower) PL spectra from an aqueous suspension of HiPco SWNTs. Both spectra contain transitions from eight SWNT species, each of which have been fitted with Voigt profiles (shaded) to illustrate the individual SWNT PL components.

transitions to the second and third lowest excited states, respectively. These transitions have often been labeled E_{22} and E_{33}, denoting the excitation of an electron from the second (third) highest van Hove singularity (vHS) in the valence band to the second (third) lowest vHS in the conduction band. Recent calculations[29] of the density of single particle states for (8,0) SWNTs has demonstrated that this simple arrangement of vHSs does not always hold and the lowest energy optically allowed transition may not necessarily occur between ν_1 and c_1. Following Spataru *et al.*,[29] excited states will be denoted, in order of increasing energy, as A_0, B_0, and C_0.

Two streaks associated with Raman lines are clearly visible in the upper right corner of the image (b) in Fig. 1; these are 200 and 325 meV (1613 and 2621 cm^{-1}) from the excitation line and their intensities can be fitted to Lorentzian functions with widths at half maximum of 18 ± 0.5 and 23 ± 0.5 meV, respectively. They represent[34,35] the tangential C-C SWNT stretching G modes and the first overtone, G', of the disorder (D) modes. When the data are plotted with a logarithmic intensity scale another Raman line can be identified at 523 meV (4218 cm^{-1}), which corresponds to the $G'+G$ combination mode.

Two typical PL slices from the 2D data in Fig. 1 are replotted for further analysis in Fig. 2. The upper spectrum was produced by resonant excitation of the B_0 exciton in (6,5) tubes at 565 nm, and the lower spectrum shows a typical nonresonant spectrum after 600 nm excitation. Neither Lorentzian nor Gaussian profiles gave convincing fits to the recorded PL data, indicating that homogeneous and inhomogeneous broadening mechanisms, which would contribute Lorentzian and Gaussian character, respectively, to the PL peaks, are of roughly the same magnitude. Purely Lorentzian line shapes have been observed in previous PL studies on single nanotubes at 4 K[16] and at room temperature,[17] and, in both cases, multiple peaks appeared over a spectral range where bands had previously been observed and assigned to nanotubes with common chirality. It therefore seems likely that, in addition to room-temperature broadening, the Gaussian components that appear in our SWNT PL data arise because of local variations in the solvent and/or surfactant environment experienced by tubes with a given (n,m) assignment.(See e.g. Ref 34).

The shape of the SWNT PL from each SWNT species was modeled using Voigt profiles,[36,37] which allowed the relative contributions of Lorentzian and Gaussian components to be estimated. The Voigt profile is given by

$$P(x,y) = \frac{1}{\alpha_G}\sqrt{\frac{\ln 2}{\pi}}K(x,y), \tag{1}$$

where $K(x,y)$, called the "Voigt function," is given by

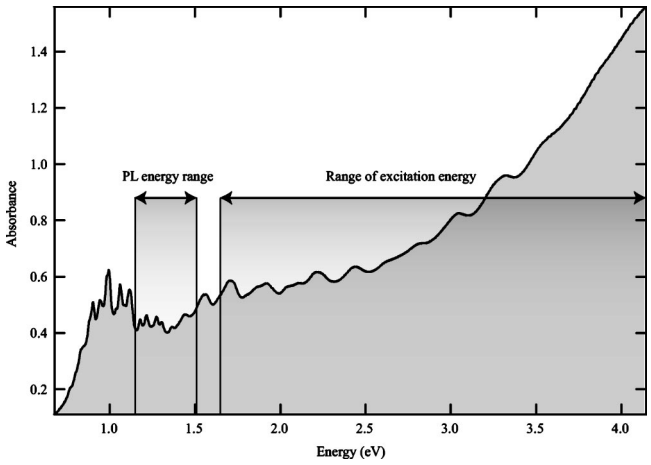

FIG. 3. The absorption spectrum of HiPco SWNTs suspended in water using SDS surfactant (1 wt %). The emission and excitation energy ranges that define the axes in Fig. 1 are highlighted.

$$K(x,y) = \frac{y}{\pi}\int_{-\infty}^{\infty} \frac{\exp(-t^2)}{y^2 + (x-t)^2}dt$$

$$\text{where } x = \frac{\nu - \nu_0}{\alpha_G}\sqrt{\ln 2}, \quad y = \frac{\alpha_L}{\alpha_G}\sqrt{\ln 2}, \qquad (2)$$

and where α_L and α_G are the half widths of the Lorentzian and Gaussian components, respectively.

When y, proportional to the ratio of Lorentzian to Gaussian widths, was assumed to be the same for each peak, the PL profiles of eight nanotube species could be simultaneously modeled in each of the 450 PL spectra displayed in Fig. 1. The shaded peaks in Fig. 2 represent these fitted Voigt PL profiles. It should be noted that while the amplitudes of these functions vary, their positions (ν_0) and widths (α_L and α_G) remain essentially unchanged over the entire 2D PL spectrum. From these fits, the full widths at half maximum of the SWNT PL were extracted and found to be: 10.2 ± 3.2 meV and 19.2 ± 3 meV for the deconvoluted Lorentzian and Gaussian components, respectively. The errors on α_L and α_G are $2 \times \sigma$, where σ is the standard deviation of α_L and α_G calculated over all 450 PL spectra. By an approximation given by Whiting,[38] the Voigt widths at half maximum are calculated to be 30.2 ± 1.4 meV which are consistent with previous ensemble measurements.[7,39]

Photoluminescence from the (11,0) and (7,3) nanotubes contributes shoulders to the (10,2) and (6,5) PL peaks, respectively, in Fig. 1; however, their inclusion in the PL fitting procedure was found to be essential to obtain a consistently good fit over the entire excitation wavelength range. Indeed, the PL contribution from the (7,3) tubes was initially neglected until the fit residuals dictated that an additional Voigt profile was required.

The SWNT absorption spectrum is presented in Fig. 3 and the excitation and emission energy ranges used to produce the PL spectra in Fig. 1 are highlighted. The absorption features that lie within the PL energy range mirror peaks in the PL data, so by superimposing absorption and PL plots, the Stokes shift of emission with respect to absorption energies can be extracted for the SWNT species whose absorption lines are narrow and distinct. This process is depicted in Fig. 4 and the data are presented in Table I. The Stokes shifts are very small (<8 meV) for (10,2), (7,5), (6,5), and (8,3) tubes and are in agreement with previously measured values.[7,22,40] This indicates that the distribution of the nuclear coordinates is little affected by photoexcitation into the A_0 state; i.e., there is very little reorganization of SWNT structure and

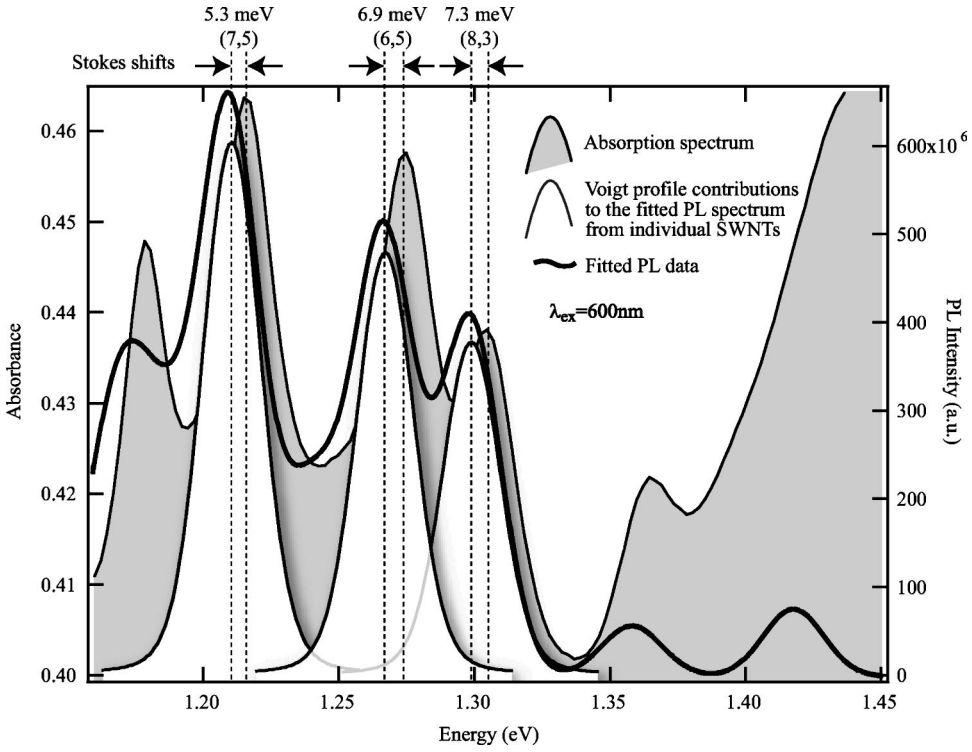

FIG. 4. A comparison of PL and absorption spectra within the PL energy range defined in Fig. 3. Also shown are three of the Voigt profiles corresponding to the PL contributions from the (7,5), (6,5), and (8,3) tubes. Values of the Stokes shifts for these SWNT species are calculated from the energies of their Voigt PL contributions and the positions of the corresponding absorption peaks.

TABLE I. SWNT PL, absorption, and Stokes shift energies.

SWNT species	Diameter (d/nm)	PL energy (eV)	Stokes shift ($\pm 2\sigma$) (meV)	B_0 PLE energy [$E(B_0)$/eV]	B_1 subpeak offset, $\Delta = E(B_1) - E(B_0)$ (meV)	C_0 PLE energy [$E(C_0)$/eV]
(6,4)	0.692	1.4188		2.1361	209	3.815
(7,3)	0.706	1.2424		2.4522	234	
(6,5)	0.757	1.2673	6.9±0.6	2.1887	229	3.606
(9,1)	0.757	1.3583		1.7916		3.375
(8,3)	0.782	1.2987	7.3±0.4	1.8686	211	3.515
(7,5)	0.829	1.2110	5.3±1.0	1.9249	230	3.683
(11,0)	0.873	1.1942		1.6693	206	3.281
(10,2)	0.884	1.1730	5.2±2.8	1.6894	215	3.358

surrounding solvent and/or surfactant molecules. This means that the difference in the magnitudes of the coupling between electronic and vibrational states (electron-lattice coupling) between the ground and excited states is small, resulting in a Huang-Rhys parameter (S) close to zero. It is not yet clear how the Stokes shift depends on surfactant; however, a recent report by Moore *et al.*[13] highlighted absolute shifts in both absorption and emission energies with different surfactants. While the Stokes shift values may not be affected by surfactant, these energy shifts could confirm the effect of the local dielectric constant on exciton binding energy reported by Perebeinos *et al.*[41]

The strong Lorentzian component to the line shapes, which is observed in the PL spectra, complements the observation of a small Stokes shift. An electronic system may be coupled to a number of vibrational modes, including intramolecular vibrations as well as "bath" modes such as local intermolecular modes and collective solvent modes. Nuclear motions that couple to an electronic transition can often be modeled as independent harmonic modes whose equilibrium position is displaced between the two electronic states. When nuclear dynamics are fast compared with the coupling strength (the fast modulation limit)[42,43] the electronic transition is effectively decoupled from the bath (solvent and surfactant), the line shapes of absorption and emission are expected to assume a Lorentzian form, and the Stokes shift will vanish. Moving away from this limit, an electronic system that is coupled to just a few independent degrees of freedom, such as the few allowed intermolecular vibrations (rather than a continuous distribution of oscillators), develops absorption and emission line shapes with Voigt profiles.[44] This is clearly what is seen in the micellar-suspended SWNT PL and is suggestive of weak coupling of the exciton with surrounding molecules and of a prominent intrananotube electronic dephasing mechanism.

Time-resolved PL was measured in (6,5), (7,5), and (8,3) SWNTs by setting $\lambda_{ex}/\lambda_{em}$ to 565/978, 643/1024, and 662/955 nm, respectively. The PL decay of the (7,5) tubes is presented in Fig. 5 together with the instrument response function (IRF). The data were analyzed, as described in the previous section, by convolution of a model decay function with the IRF.[31] The analysis was performed over the full time range of the decay (0–10 ns in Fig. 5) and the features in the decay at 5 ns and 9 ns were due to photomultiplier effects.[45] Acceptable fits were obtained when a double exponential model decay function, $I_{PL}(t) = \alpha_1 \exp(-t/\tau_1) + \alpha_2 \exp(-t/\tau_2)$, was used, and the resulting fit is shown by the solid line in Fig. 5. The fractional contribution Y_n that each decay time τ_n constitutes to the steady-state PL intensity[46] is presented, along with values for τ_n and α_n in the inset table. The errors in the values of τ_n are $2\times\sigma$, where σ is the standard deviation of τ_n. Although the fractional contribution of τ_2 is only 1%, force fitting the data to one exponential decay was found to add significant uncertainty to the value of τ_1.

A short lifetime component of ~130 ps is found to dominate ($Y_n = 99\%$) in each of the three tube types. This is considerably longer than the 5–15 ps decay times measured in previous studies,[22,26] and Ma *et al.*[24] have suggested that a strong dependence of PL lifetime on pump intensity could be described by an exciton-exciton annihilation model. The excitation intensity used to generate the data here ($1.4–1.7 \times 10^{12}$ photons pulse^{-1} cm^{-2}) is $10^2–10^4$ times less intense than the intensities used by Ma *et al.*[24] and, by extrapolating their results, less than one exciton is generated per tube in our experiments. Thus, we expect there to be almost no exciton-exciton annihilation. Any fast (5–15 ps) decays would be readily resolvable in our experiment since the reconvolution procedure reliably extracts features that are 5–10% of the instrument response function width (~200 ps).[31] The shift between the peaks of the IRF and the PL decay curves arises because the IRF has a finite width, and it is not indicative of a PL rise time.

Natural radiative lifetimes of SWNTs can be obtained if the PL lifetime and PL quantum yield (PLQY) are known. The PLQY, ϕ_{PL}, can be calculated for the ensemble when the full PL spectrum has been recorded or for individual tube species when their individual contributions to the PL and absorption spectra can be estimated. The former measurement, on aqueous solutions of HiPco SWNTs, has been reported to be $\sim 10^{-3}$ by O'Connell *et al.*[7] and 1.7×10^{-4} by Wang *et al.*;[26] however, since the data presented in our study cover a subset of the total SWNT population, the calculation of two single-tube ϕ_{PL} values are presented. The method for obtaining the contributions of individual semiconducting tubes to the ensemble PL has already been described (see Fig. 2), and a similar fitting method can be used to extract

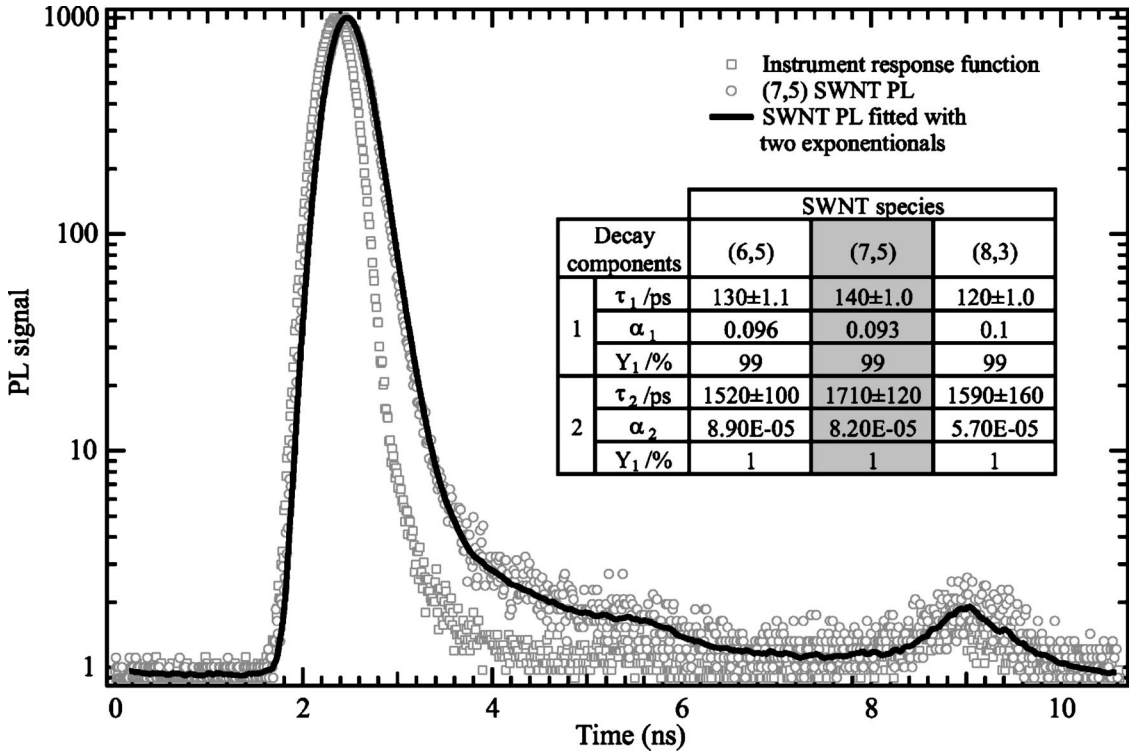

Decay components		SWNT species (6,5)	(7,5)	(8,3)
1	τ_1 /ps	130±1.1	140±1.0	120±1.0
	α_1	0.096	0.093	0.1
	Y_1 /%	99	99	99
2	τ_2 /ps	1520±100	1710±120	1590±160
	α_2	8.90E-05	8.20E-05	5.70E-05
	Y_1 /%	1	1	1

FIG. 5. Instrument response function (IRF) and luminescence decay profile from (7,5) SWNTs. The solid line corresponds to the IRF convoluted with a biexponential decay function. The inset table presents the corresponding lifetimes and yields of each function used to fit the PL from the (6,5), (7,5), and (8,3) SWNTs.

their contributions to the absorption spectrum; however, both the residual carbonaceous impurities and the tail of the SWNT π-plasmon resonance, whose peak lies at around 5 eV,[47–49] contribute to a significant absorption background that usually contributes more than 70% of the optical density at the first absorption band of metallic tubes.[20] Figure 6 shows a portion of the % absorption spectrum, containing transitions to the B_0 exciton, which has been fitted with Voigt functions offset from zero by a linear background function that approximates the π-plasmon tail. The two highlighted Voigt functions in Fig. 6 are located at the energies of the B_0 exciton photoluminescence excitation (PLE) peaks of (8,3)

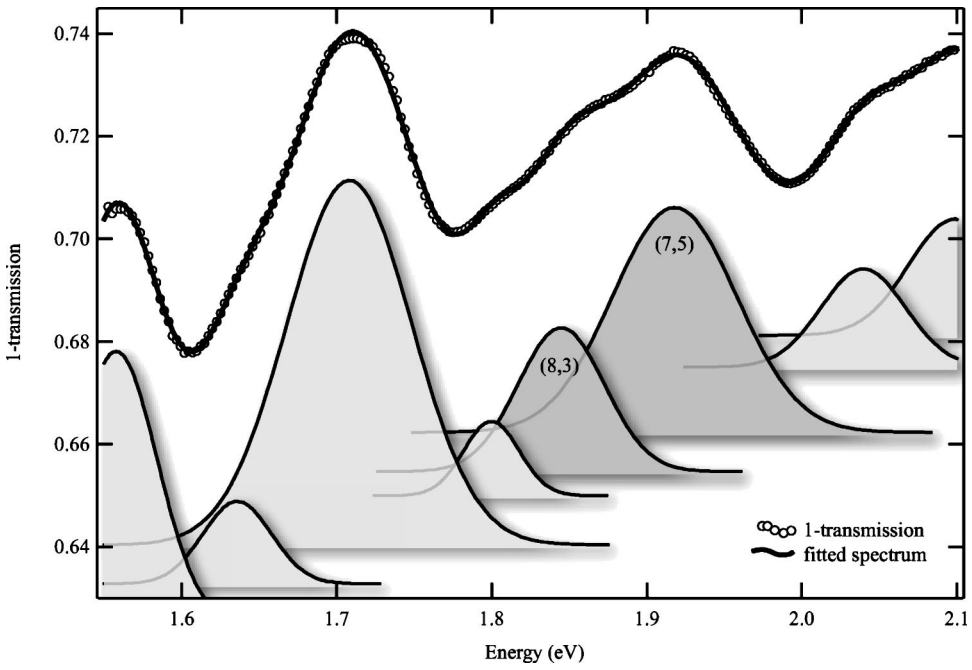

FIG. 6. A section of the fitted % absorption spectrum containing transitions to the B_0 states of semiconducting SWNTs. The Voigt profiles that contribute to the fitted spectrum are offset from zero by a linear background correction (freely variable in the fitting procedure) that estimates the contribution of both residual carbonaceous impurities and the SWNT π-plasmon resonance to the optical density.

and (7,5) tubes (see Table I) and are therefore assigned to the absorption contributions of these tubes.

Integrated PL intensities of (8,3) and (7,5) tubes were compared to a standard, perylene dye, Lumogen™ F Red 300, with a PLQY of 100%. The resulting quantum yields were found to be $\sim 5 \times 10^{-4}$ for both (8,3) and (7,5) tubes, about half the ensemble value reported by O'Connell *et al.*[7] In order to make this determination, we assume that the B_0 exciton relaxed to the emissive A_0 exciton state with unit quantum efficiency. Given the relationship between PLQY and the natural radiative and measured PL lifetimes, τ_r and τ_{PL} ($\phi_{PL} = \tau_{PL}/\tau_r$), we conclude that $\tau_r \approx 260$ ns. The relatively slow time constant suggests that the transition is not fully, radiatively allowed; however, this is inconsistent with the observation of a strong absorption coefficient and a small Stokes shift. This discrepancy would be alleviated if the observed PLQY was, in fact, less than the "true" PLQY, leading to the conclusion that the majority of (8,3) and (7,5) SWNTs that absorb photons do not produce PL. This might be the case if SWNTs exist in bundles containing one or more metallic tubes. The PL was reduced by quenching for all but those semiconducting tubes that are truly isolated from metallic tubes. As suggested by Ma *et al.*,[24] the quantum efficiency for formation of the A_0 exciton after excitation of the B_0 exciton may be less than unity, which would also reduce the calculated PLQY values in all experiments such as this one, in which the A_0 exciton is not excited directly.

If it is assumed that the transition is fully allowed, then an estimate of the natural radiative lifetime can be made. When combined with the measured PL lifetime this would yield a value for the true PLQY of isolated SWNTs. For a strongly emissive dye that emits at 598 nm, the natural radiative lifetime has been determined to be 4.14 ns.[50] Taking the cubic dependence[51] of the natural radiative lifetime on transition wavelength, the (7,5) SWNT that emits 1024 nm would be predicted to have a value of 20 ns. Combining this value with the measured SWNT PL lifetime of 130 ps, the PLQY of a sample of perfectly unbundled (7,5) SWNTs would be $\sim 6.5 \times 10^{-3}$. We therefore conclude that the ratio of the measured PLQY to this value is in fact a more reasonable measure of the proportion of single vs bundled SWNTs in solution.

PLE spectra for individual SWNT species were produced by integration of the fitted PL Voigt profiles at each excitation wavelength. A PLE spectrum produced in this way con-

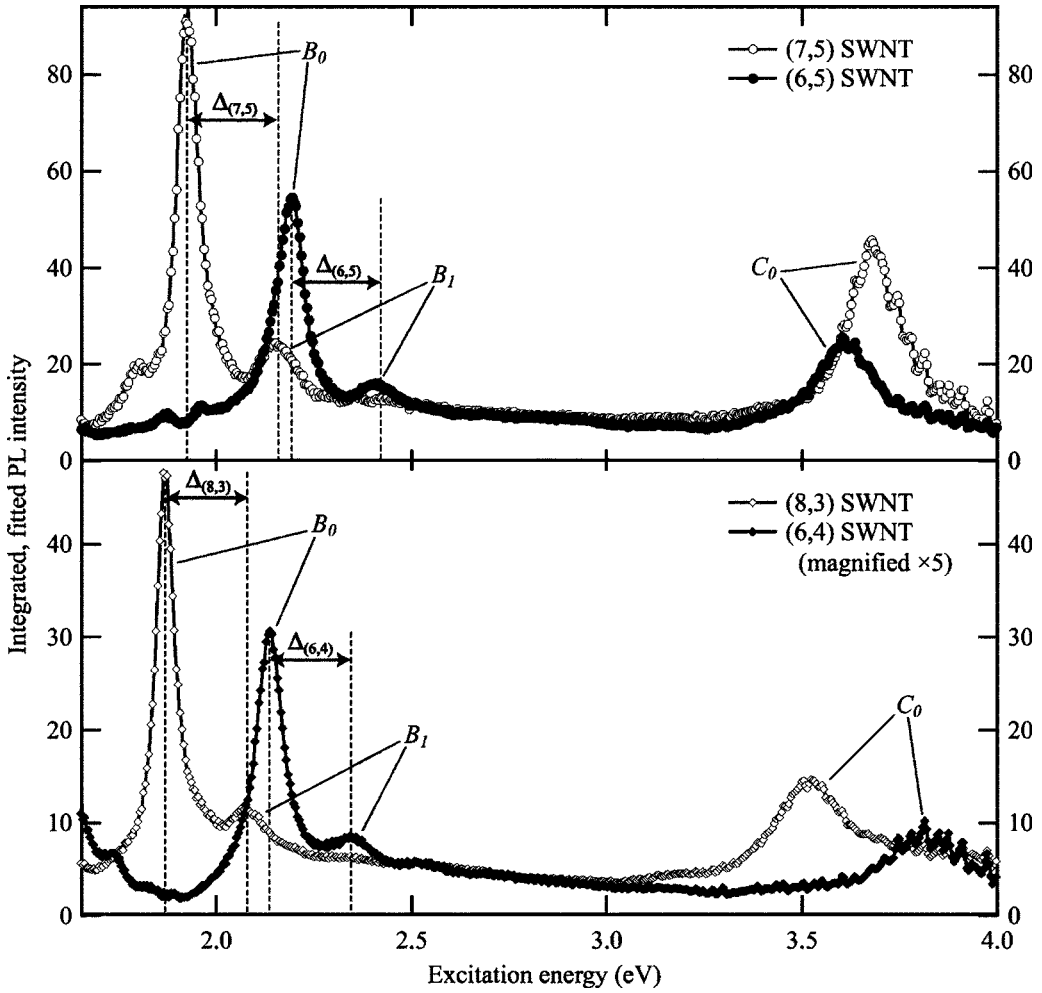

FIG. 7. Normalized excitation spectra for the (7,5), (6,5), (8,3), and (6,4) SWNTs. PL due to excitation of the B_0 and C_0 excitons is clearly observed. The peak labeled B_1 is a subpeak associated with B_0 for all observed SWNT species.

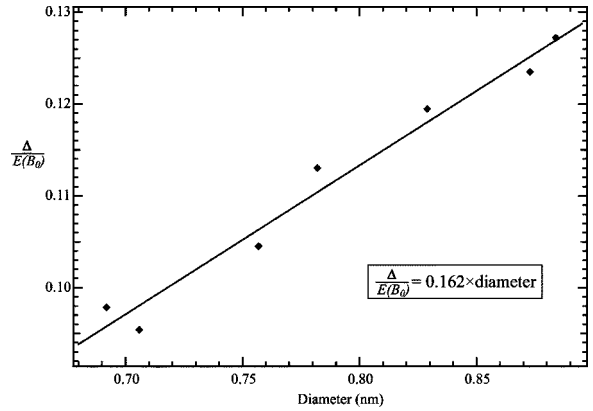

FIG. 8. Showing the linear relationship between $\Delta/E(B_0)$ and tube diameter, where $\Delta = E(B_1) - E(B_0)$.

tains only the emission from the tube type of interest and is superior to PLE spectra produced by taking vertical slices down Fig. 1 since these would contain signals from all tubes whose PL overlaps those slices. Figure 7 shows the normalized excitation spectra of four SWNT species: (7,5), (6,5), (8,3), and (6,4). In each of the spectra the PL due to excitation of the B_0 and C_0 excitons is clearly observed and appears to be Lorentzian in character.

Associated with the B_0 exciton PLE peak is a subpeak, labeled B_1, which is shifted by $\sim$200 meV from the main peak. The energy offset, Δ, of this peak from its parent peak has been extracted from these data for seven tube species and, as illustrated in Fig. 8, it is found that there is an approximately linear relationship between $\Delta/E(B_0)$ and d, where $E(B_0)$ is the energy of the B_0 exciton PLE peak and d is the SWNT diameter. Values of $E(B_0)$, $E(C_0)$, and Δ are presented in Table I.

The subpeaks, B_1, could either constitute a coupling of the electronic transition with a vibrational mode associated with the B_0 state (a vibronic transition) or could arise via a transition to an excited excitonic state. Considering the latter case, an exciton can often exist in a number of nonground state configurations that retain a correlated e^-h^+ pair. Recent calculations[29] have predicted that such states exist in an (8,0) SWNT, although their absorption cross section is likely to be very low. According to these calculations, $\Delta/E(B_0) \approx 0.33$ in an (8,0) tube and $d \approx 0.635$ nm, which, when plotted on the graph in Fig. 8, would fall far from the extrapolated line.

Considering the vibronic case, it is interesting to note that the magnitude of Δ ($205 < \Delta < 235$ meV) is reminiscent of and slightly greater than both SWNT tangential C-C stretching G modes[35] and the E_{2g} Raman active modes of graphite (195.3 meV),[52] both of which are ground state vibrational modes. The Stokes shift and PL line shape data point to minimal SWNT distortion upon excitation, so corresponding vibrational modes in the B_0 state are expected to resonate at similar frequencies. Indeed, excitation of an electron from a bonding to an antibonding orbital in the conduction band might be expected to weaken nearby C-C bonds and actually reduce the frequency of the tangential modes relative to the Raman active ground state modes. The B_1 subpeaks may therefore correspond to excitation of bands that are either E_{2g} bands combined with low frequency, radial breathing modes, or other vibrational modes that are not observed using Raman spectroscopy. Unfortunately, there appears to be no conclusive evidence to attach a firm assignment to the B_1 subpeaks.

How can the linear relationship between $\Delta/E(B_0)$ and d be explained? The energies of transitions to A_0, B_0, and C_0 states tend to decrease with increasing d;[33,53] however, when d is small, there is a large dependence of the transition energy on chiral angle, θ, which is known as trigonal warping.[54,55] It is found that only SWNTs having n-m as a constant integer have transition energies that have a smooth, functional dependence on d. When plotted separately against tube diameter, neither $E(B_0)$ or Δ appear to follow simple trends, indicating that θ has a strong affect on the electronic properties of tubes in this diameter range; however, when Δ is divided by $E(B_0)$ the angular dependence appears to cancel out, leaving a component that is proportional to diameter.

IV. CONCLUSIONS

Upon detailed analysis, the PL spectra of HiPco SWNTs, excited at multiple wavelengths, yield interesting information about ground and excited states. Small Stokes shifts and the observation of Lorentzianlike line shapes suggests that the exciton couples weakly with surrounding solvent and surfactant molecules and dephases via a predominantly intrananotube mechanism. A PL lifetime of $\sim$130 ps has been measured for (7,5), (8,3), and (6,5) SWNTs and the PL quantum efficiency of (7,5) and (8,3) tubes has been estimated to be $\sim 5 \times 10^{-4}$. These measurements yield a long natural radiative lifetime of 260 ns that is inconsistent with a strong absorption coefficient and a small Stokes shift. The quenching of semiconducting SWNT PLs by association with metallic SWNTs in tube bundles probably yields PLQY measurements that are much smaller than the true values because these bundles contribute to absorption but not to PL. In addition, the PLQY measurements would be lowered if the quantum efficiency for the relaxation of the B_0 exciton to form the emitting A_0 exciton was less than unity. By choosing a suitable value for the natural radiative lifetime of fully allowed transition, an estimate of the true PLQY of $\sim 6.5 \times 10^{-3}$ has been made. SWNT samples that are dispersed more effectively in solution are expected to exhibit higher PL quantum efficiencies with values that asymptotically approach this value. Finally, extraction of tube-specific excitation spectra clearly reveals vibrational bands that are associated with the second (B_0) excitonic state. It is found that there is a linear relationship between $\Delta/E(B_0)$ and d, where Δ is the energy difference between the vibronic band and the energy of the B_0 state, $E(B_0)$, in a tube of diameter, d.

ACKNOWLEDGMENT

This work was funded by the U.S. Department of Energy, Office of Science, Basic Energy Sciences, Chemical Sciences, Geosciences, and Biosciences Division, under Contract No. DE-AC36-99GO10337 to NREL.

[1] S. Iijima, Nature (London) **354**, 56 (1991).
[2] M. M. J. Treacy, T. W. Ebbesen, and J. M. Gibson, Nature (London) **381**, 678 (1996).
[3] P. Kim, L. Shi, A. Majumdar, and P. L. McEuen, Phys. Rev. Lett. **87**, 215502 (2001).
[4] A. Bachtold, M. S. Fuhrer, S. Plyasunov, M. Forero, E. H. Anderson, A. Zettl, and P. L. McEuen, Phys. Rev. Lett. **84**, 6082 (2000).
[5] W. J. Liang, M. Bockrath, D. Bozovic, J. H. Hafner, M. Tinkham, and H. Park, Nature (London) **411**, 665 (2001).
[6] Z. Yao, C. Dekker, and P. Avouris, in *Electrical Transport Through Single-Wall Carbon Nanotubes* (Springer-Verlag, Germany, 2001), Vol. 80, p. 147.
[7] M. J. O'Connell, S. M. Bachilo, C. B. Huffman, V. C. Moore, M. S. Strano, E. H. Haroz, K. L. Rialon, P. J. Boul, W. H. Noon, C. Kittrell, J. P. Ma, R. H. Hauge, R. B. Weisman, and R. E. Smalley, Science **297**, 593 (2002).
[8] S. M. Bachilo, M. S. Strano, C. Kittrell, R. H. Hauge, R. E. Smalley, and R. B. Weisman, Science **298**, 2361 (2002).
[9] R. B. Weisman, S. M. Bachilo, and D. Tsyboulski, Appl. Phys. A: Mater. Sci. Process. **78**, 1111 (2004).
[10] M. J. Bronikowski, P. A. Willis, D. T. Colbert, K. A. Smith, and R. E. Smalley, J. Vac. Sci. Technol. A **19**, 1800 (2001).
[11] S. Lebedkin, K. Arnold, F. Hennrich, R. Krupke, B. Renker, and M. M. Kappes, New J. Phys. **5**, 140 (2003).
[12] S. Lebedkin, F. Hennrich, T. Skipa, and M. M. Kappes, J. Phys. Chem. B **107**, 1949 (2003).
[13] V. C. Moore, M. S. Strano, E. H. Haroz, R. H. Hauge, R. E. Smalley, J. Schmidt, and Y. Talmon, Nano Lett. **3**, 1379 (2003).
[14] J. Lefebvre, J. M. Fraser, Y. Homma, and P. Finnie, Appl. Phys. A: Mater. Sci. Process. **78**, 1107 (2004).
[15] J. Lefebvre, J. M. Fraser, P. Finnie, and Y. Homma, Phys. Rev. B **69**, 075403 (2004).
[16] H. Htoon, M. J. O'Connell, P. J. Cox, S. K. Doorn, and V. I. Klimov, Phys. Rev. Lett. **93**, 027401 (2004).
[17] A. Hartschuh, H. N. Pedrosa, L. Novotny, and T. D. Krauss, Science **301**, 1354 (2003).
[18] J. Lefebvre, P. Finnie, and Y. Homma, Phys. Rev. B **70**, 045419 (2004).
[19] J. S. Lauret, C. Voisin, G. Cassabois, C. Delalande, P. Roussignol, L. Capes, and O. Jost, Physica E (Amsterdam) **17**, 380 (2003).
[20] J. S. Lauret, C. Voisin, G. Cassabois, C. Delalande, P. Roussignol, O. Jost, and L. Capes, Phys. Rev. Lett. **90**, 057404 (2003).
[21] J. Kono, G. N. Ostojic, S. Zaric, M. S. Strano, V. C. Moore, J. Shaver, R. H. Hauge, and R. E. Smalley, Appl. Phys. A: Mater. Sci. Process. **78**, 1093 (2004).
[22] A. Hagen, G. Moos, V. Talalaev, and T. Hertel, Appl. Phys. A: Mater. Sci. Process. **78**, 1137 (2004).
[23] O. J. Korovyanko, C. X. Sheng, Z. V. Vardeny, A. B. Dalton, and R. H. Baughman, Phys. Rev. Lett. **92**, 017403 (2004).
[24] Y. Z. Ma, J. Stenger, J. Zimmermann, S. M. Bachilo, R. E. Smalley, R. B. Weisman, and G. R. Fleming, J. Chem. Phys. **120**, 3368 (2004).
[25] G. N. Ostojic, S. Zaric, J. Kono, M. S. Strano, V. C. Moore, R. H. Hauge, and R. E. Smalley, Phys. Rev. Lett. **92**, 117402 (2004).
[26] F. Wang, G. Dukovic, L. E. Brus, and T. F. Heinz, Phys. Rev. Lett. **92**, 177401 (2004).
[27] T. Ando, J. Phys. Soc. Jpn. **66**, 1066 (1997).
[28] C. L. Kane and E. J. Mele, Phys. Rev. Lett. **90**, 207401 (2003).
[29] C. D. Spataru, S. Ismail-Beigi, L. X. Benedict, and S. G. Louie, Appl. Phys. A: Mater. Sci. Process. **78**, 1129 (2004).
[30] C. D. Spataru, S. Ismail-Beigi, L. X. Benedict, and S. G. Louie, Phys. Rev. Lett. **92**, 077402 (2004).
[31] D. V. O'Connor and D. Phillips, *Time-Correlated Single Photon Counting* (Academic Press, New York, 1984).
[32] D. W. Marquardt, J. Soc. Ind. Appl. Math. **11**, 431 (1963).
[33] R. B. Weisman and S. M. Bachilo, Nano Lett. **3**, 1235 (2003).
[34] A. M. Rao, E. Richter, S. Bandow, B. Chase, P. C. Eklund, K. A. Williams, S. Fang, K. R. Subbaswamy, M. Menon, A. Thess, R. E. Smalley, G. Dresselhaus, and M. S. Dresselhaus, Science **275**, 187 (1997).
[35] P. H. Tan, Y. Tang, Y. M. Deng, F. Li, Y. L. Wei, and H. M. Cheng, Appl. Phys. Lett. **75**, 1524 (1999).
[36] B. H. Armstrong, J. Quant. Spectrosc. Radiat. Transf. **7**, 61 (1967).
[37] J. Humlicek, J. Quant. Spectrosc. Radiat. Transf. **27**, 437 (1982).
[38] E. E. Whiting, J. Quant. Spectrosc. Radiat. Transf. **8**, 1379 (1968).
[39] J. Lefebvre, Y. Homma, and P. Finnie, Phys. Rev. Lett. **90**, 217401 (2003).
[40] M. S. Arnold, J. E. Sharping, S. I. Stupp, P. Kumar, and M. C. Hersam, Nano Lett. **3**, 1549 (2003).
[41] V. Perebeinos, J. Tersoff, and P. Avouris, Phys. Rev. Lett. **92**, 257402 (2004).
[42] R. Kubo, Adv. Chem. Phys. **15**, 101 (1969).
[43] R. Kubo, in *Fluctuation Relaxation and Resonance in Magnetic Systems*, edited by D. Ter Haar (Oliver and Boyd, Edinburgh, 1962).
[44] S. Mukamel, *Principles of Nonlinear Optical Spectroscopy* (Oxford University Press, Oxford, 1995).
[45] C. Lewis, W. R. Ware, L. J. Doemeny, and T. L. Nemzek, Rev. Sci. Instrum. **44**, 107 (1973).
[46] J. R. Lakowicz, *Principles of Fluorescence Spectroscopy* (Kluwer Academic/Plenum Publishers, New York, 1999).
[47] T. Pichler, M. Knupfer, M. S. Golden, J. Fink, A. Rinzler, and R. E. Smalley, Phys. Rev. Lett. **80**, 4729 (1998).
[48] M. E. Itkis, S. Niyogi, M. E. Meng, M. A. Hamon, H. Hu, and R. C. Haddon, Nano Lett. **2**, 155 (2002).
[49] S. Kazaoui, N. Minami, H. Kataura, and Y. Achiba, Synth. Met. **121**, 1201 (2001).
[50] J. L. Clark, P. F. Miller, and G. Rumbles, J. Phys. Chem. A **102**, 4428 (1998).
[51] S. J. Strickler and R. A. Berg, J. Chem. Phys. **37**, 814 (1962).
[52] F. Tuinstra and J. L. Koenig, J. Chem. Phys. **53**, 1126 (1970).
[53] H. Kataura, Y. Kumazawa, Y. Maniwa, I. Umezu, S. Suzuki, Y. Ohtsuka, and Y. Achiba, Synth. Met. **103**, 2555 (1999).
[54] R. Saito, G. Dresselhaus, and M. S. Dresselhaus, Phys. Rev. B **61**, 2981 (2000).
[55] S. Reich and C. Thomsen, Phys. Rev. B **62**, 4273 (2000).